AAS 21-270

QUASI-PERIODIC ORBITS IN THE SUN-EARTH-MOON BICIRCULAR RESTRICTED FOUR-BODY PROBLEM

Brian P. McCarthy* **and Kathleen C. Howell†**

Examining the properties of quasi-periodic orbits provides insight into the Sun-perturbed environment in cislunar space. In this investigation, quasi-periodic trajectories and their properties are explored in a Sun-Earth-Moon Bicircular Restricted Four-Body Problem (BCR4BP). Additionally, computation and stability of invariant torus families in the BCR4BP are detailed. Understanding quasi-periodic behavior in the BCR4BP expands available options for path planning to destinations in the lunar vicinity.

INTRODUCTION

In 2020, NASA released the agency's lunar exploration program overview, offering the latest Artemis and Gateway status as well as plans for additional extended lunar missions.[1] To enable both of these endeavors, an understanding of the multi-body dynamical environment is crucial to the success of the program. However, given the chaotic nature of the dynamical behaviors in a multi-body system, preliminary path planning in this environment is time-intensive and computationally unwieldy. To meet these challenges, the underlying dynamical structures available in cislunar space can aid in creating viable mission options and in streamlining the trajectory design process. Investigations into disposal dynamics and low-energy transfers reveal that solar gravity is also a significant force in preliminary trajectory design in cislunar space.[2–4] To support design in a regime where all three bodies significantly influence the path of a vehicle, quasi-periodic orbits in the Bicircular Restricted Four-Body Problem (BCR4BP) are examined. The BCR4BP serves as a useful model for preliminary trajectory design where the complex dynamics in both the Earth-Moon and Sun-Earth regimes are significant. In contrast to periodic orbits in the BCR4BP, quasi-periodic trajectories exist in families of solutions in this model. Additionally, incorporating quasi-periodic orbits from the BCR4BP during the design process reveals natural motion that is not captured within an Earth-Moon or Sun-Earth three-body system. This investigation examines the existence of quasi-periodic orbits in the BCR4BP, characterizes their stability, and expands the families of orbits. Computational techniques are presented to highlight challenges associated with the process of computing families of quasi-periodic orbits in the BCR4BP. Quasi-periodic orbits, while more computationally intensive to produce than periodic orbits, build out the framework of the dynamical structures that can be incorporated into the trajectory design process in the Sun-Earth-Moon system.

*Ph.D. Student, School of Aeronautics and Astronautics, Purdue University, West Lafayette, IN 47907; mccart71@purdue.edu

†Hsu Lo Distinguished Professor of Aeronautics and Astronautics, School of Aeronautics and Astronautics, Purdue University, West Lafayette, IN 47907; howell@purdue.edu

DYNAMICAL MODEL

The model examined in this investigation is the BCR4BP. In the BCR4BP, the gravitational forces from the Sun, Earth, and Moon are incorporated into a single model while reducing the complexity as compare to an ephemeris model. The BCR4BP describes the motion of an infinitesimal mass (P_3) under the influence of three massive bodies, the Earth (P_1), Moon (P_2), and Sun (P_4). The Earth and Moon move in circular paths about their mutual barycenter, denoted B_1. Similarly, the Sun and B_1 move in circular, Keplerian motion about their mutual barycenter, B_2. This formulation of the four-body problem is not coherent, i.e., the motion of the Earth and Moon are not perturbed further by solar gravity. Additionally, it is assumed that the Earth-Moon orbital plane is the same plane as the Sun-B_1 orbit plane; although not necessary, such an assumption is adequate for this analysis. The model is defined relative to a rotating coordinate system, where the $+\hat{x}$-direction is defined from Earth (P_1) to the Moon (P_2). The $+\hat{z}$-direction is defined in the direction of the orbital angular momentum for the Earth and Moon; the $+\hat{y}$-direction completes the orthonormal triad. The BCR4BP is a time dependent system, where the location of the Sun in the Earth-Moon rotating frame is defined by a single angle, θ_S. The Sun moves in a clockwise direction about B_1 (i.e., $\dot{\theta}_S$ is negative), as illustrated in Figure 1(a). The equations of motion that describe the motion of the massless particle, P_3, in the Earth-Moon rotating frame are defined,

$$\ddot{x} = 2\dot{y} + \frac{\partial \Upsilon}{\partial x} \qquad (1) \qquad\qquad \ddot{y} = -2\dot{x} + \frac{\partial \Upsilon}{\partial y} \qquad (2) \qquad\qquad \ddot{z} = \frac{\partial \Upsilon}{\partial z} \qquad (3)$$

Note that Υ is the pseudo-potential in the BCR4BP in the Earth-Moon rotating frame. It is defined as,

$$\Upsilon = \frac{1-\mu}{r_{13}} + \frac{\mu}{r_{23}} + \frac{x^2+y^2}{2} + \varepsilon\left(\frac{m_4}{r_{43}} - \frac{m_4}{a_4^3}(x_4 x + y_4 y + z_4 z)\right) \qquad (4)$$

where x_i, y_i, and z_i are the position components of P_i relative to the barycenter in the Earth-Moon rotating frame, μ is the Earth-Moon mass parameter, $\mu = \frac{M_2}{M_1+M_2}$ (where the term M_i is defined as the mass of P_i), r_{ij} is the position magnitude of P_i relative to P_j, m_4 is the non-dimensional mass of P_4, $m_4 = \frac{M_4}{M_1+M_2}$, and a_4 is the semi-major axis of the circular orbit reflecting the Sun-B_1 motion. The term ε is a scaling parameter for the Sun mass; $\varepsilon = 0$ reflects a Circular Restricted Three-Body Problem (CR3BP) with no solar gravity and $\varepsilon = 1$ for the BCR4BP. Similarly, analyzing motion in a Sun-B_1 rotating frame is advantageous. In this frame, the $\hat{x}'$-direction is directed from the Sun to the Earth-Moon barycenter, B_1. The $\hat{z}'$-direction is defined as the direction of the Sun-B_1 orbit angular momentum; the $\hat{y}'$-direction completes the triad. The Sun-B_1 rotating frame is illustrated in Figure 1(b). It is useful to visualize motion in this frame to understand the influence of solar gravity on trajectories when excursions are encountered beyond the Earth-Moon vicinity.

Equilibrium Solutions

Instantaneous equilibrium solutions exist in the BCR4BP. By setting the first and second derivatives to zero and solving for the position, an instantaneous equilibrium solution exists for each Sun angle. A continuation process to solve for the equilibrium solutions in the BCR4BP is detailed by Boudad.[5] Since the continuum of points that represent the equilibrium solutions is dependent on Sun angle, a particle initialized at these locations will not remain there for all time. The particle immediately departs since the location of the Sun changes with time. Additionally, the motion in the vicinity of the equilibrium points is examined by using a continuation process to transition a libration point in the CR3BP to the equivalent dynamical structure in the BCR4BP. Since the BCR4BP

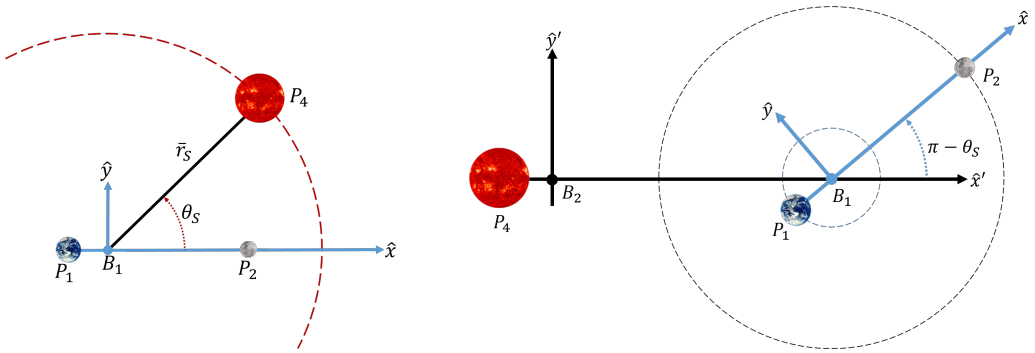

Figure 1. Earth-Moon rotating frame (left) and Sun-B_1 rotating frame (right) as defined in the BCR4BP.

is periodically forced by the Sun in the Earth-Moon rotating frame, the dynamical equivalent for a CR3BP libration point in the BCR4BP must be a periodic orbit with an orbital period equal to the synodic period. A multiple shooting differential corrections procedure is formulated using a free-variable/constraint method to compute the periodic orbits, outlined by McCarthy.[6] The free variable vector is defined,

$$\mathbf{X} = \begin{bmatrix} x_1 & y_1 & z_1 & \dots & \dot{z}_m & \dot{y}_m & \dot{z}_m & \varepsilon \end{bmatrix}^T \tag{5}$$

where m is the number of arcs in the multiple shooting scheme and ε is the parameter that scales the equations of motion from the CR3BP to the BCR4BP defined in Equation (4). The constraint vector is defined,

$$\mathbf{F} = \begin{bmatrix} x_1 - x_2 & y_1 - y_2 & \dots & \dot{y}_m - \dot{y}_1 & \dot{z}_m - \dot{z}_1 \end{bmatrix}^T \tag{6}$$

which constrains position and velocity continuity between each of the trajectory arcs. Finally, the gradient of the constraints is defined using elements of the state transition matrix by integrating an additional set of 36 equations of motion. Using a pseudo-arclength continuation strategy aids in evolving from the CR3BP ($\varepsilon = 0$) to the BCR4BP ($\varepsilon = 1$); notably, the orbit in the BCR4BP may not retain the same stability characteristics as the solution in the CR3BP. To understand possible stability changes, a hodograph that includes two parameters of the transition of the L_1 and L_2 points in the CR3BP to the BCR4BP is plotted in Figure 2. The colored segments of the hodograph indicate the stability properties across the continuation process. The horizontal axis is the pseudo arclength step size, δs. The pseudo-arclength step size is chosen as the parameter for the horizontal axis because it is monotonically increasing through the continuation process. A similar representation for the L_2 continuation hodograph was created by Rosales.[7] Blue indicates that there is a single saddle mode and two center modes, and red indicates two saddle modes and a single center mode. The L_1 continuation procedure retains consistent stability properties throughout the entire continuation process and reaches a unique solution in the BCR4BP ($\varepsilon = 1$). However, the L_2 continuation step initially transitions to $\varepsilon < 0$, then crosses back over $\varepsilon = 0$. The solution at this location where $\varepsilon = 0$ corresponds to the L_2 2:1 synodic resonant Lyapunov orbit in the CR3BP; the resonance corresponds to an orbit with 2 orbital periods for a single revolution of the Sun in the Earth-Moon rotating frame. Therefore, the orbits in the vicinity of the L_2 libration point do not necessarily transition to yield a unique structure in the BCR4BP, rather the process resets to produce the equivalent to the 2:1 synodic resonant Lyapunov orbit. This investigation focuses on the behaviors in the

vicinity of the Earth-Moon L_1 and L_2 points in the BCR4BP that result from these transitions.

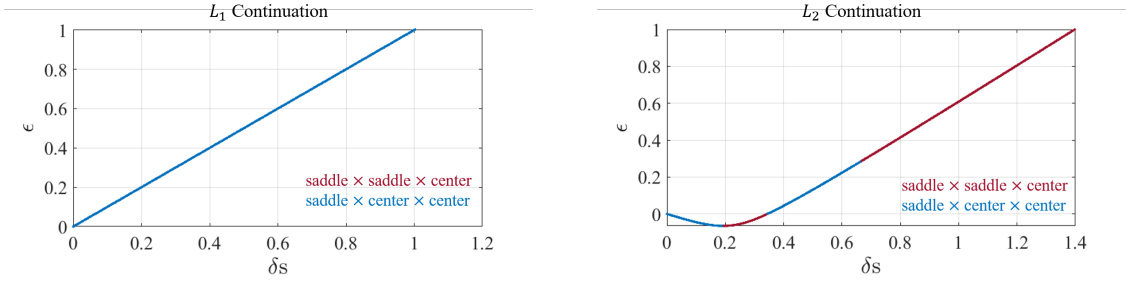

(a) (b)

Figure 2. Sun mass scaling parameter as a function of the pseudo-arclength step, δs, from the initial libration point at $\varepsilon = 0$ for (a) L_1 and (b) L_2. Note that the stability properties of the L_2 point change during the continuation process.

QUASI-PERIODIC ORBITS

Quasi-periodic orbits exist in the vicinity of periodic solutions. They are identified when the monodromy matrix possesses complex eigenvalues of unit magnitude. Furthermore, quasi-periodic trajectorties exist along families of invariant tori. Invariant tori are characterized by the number of fundamental frequencies that define the motion on the torus, such that an n-dimensional torus possesses n fundamental frequencies. Equilibrium solutions and periodic orbits are examples of 0-dimensional and 1-dimensional tori, respectively. For a periodic orbit, a single fundamental frequency defines the motion. Quasi-periodic orbits evolve on tori where $n > 1$. For non-autonomous Hamiltonian systems, one or more of the frequencies is typically constrained and the number of free variables to construct a family of invariant tori is reduced.[8] Since the BCR4BP is a periodically forced system, one of the fundamental frequencies, ω_0, is constrained to match the frequency of the system. As such, periodic orbits in the BCR4BP exist as isolated solutions because the period of the orbit must be commensurate with the synodic period of the system. Similarly, one of the frequencies reflecting a 2-dimensional quasi-periodic torus is constrained to be commensurate with the synodic period of the system and the second frequency, ω_1, is free; thus, a family of quasi-periodic orbits is defined along the frequency ω_1. Several authors have examined quasi-periodic motion in the BCR4BP previously; Jorba et al. examined quasi-periodic orbits in the vicinity of L_1 in the BCR4BP and reduction to the center manifold; Jorba and Nicolás explored quasi-periodic orbits in the vicinity of Earth-Moon L_3; Rosales investigated quasi-periodic motion in the vicinity of the Earth-Moon L_2 libration point[7,9,10] Additionally, Castellà and Jorba modelled quasi-periodic tori in the vicinity of the triangular points in the BCR4BP.[11] Given that quasi-periodic orbits are known to exist in families in the BCR4BP, they provide a wider set of options for destinations in cislunar space, relaxing the constraint of a perfectly periodic orbit. This investigation examines some properties of these quasi-periodic orbit families.

COMPUTING QUASI-PERIODIC TORI IN THE BCR4BP

Quasi-periodic orbits are known to exist in the BCR4BP. In this investigation, there are two methods used to seed an initial guess to construct solutions in the BCR4BP. The first procedure involves using the center direction computed from the monodromy matrix, similar to the process

detailed by McCarthy and Howell in the CR3BP.[12] The second approach leverages a periodic orbit in the CR3BP that is transitioned using pseudo arclength continuation from the CR3BP to the BCR4BP. Once the initial guess is constructed, a multiple shooting differential corrections strategy is employed, consistent with the steps by Gómez and Mondelo as well as Olikara and Scheeres, to compute members of a family in the BCR4BP.[13,14] This algorithm to compute a torus is defined the GMOS (Gomez-Mondelo-Olikara-Scheeres) algorithm. The behavior of the families of tori provides a broader understanding of the local Sun-perturbed cislunar environment.

Method 1: Linear Approximation of Center Direction

Generating an initial guess using the center direction associated with a periodic orbit requires computation of the eigenvalues of the monodromy matrix associated with the periodic orbit. First, the eigenvalues associated with the dynamically equivalent L_1 and L_2 orbits are computed and recorded in Table 1. Note that, in the CR3BP, there are two center modes and one saddle mode for the L_1 and L_2 libration points; however, only L_1 retains the saddle $\times$ center $\times$ center behavior for the dynamical equivalent in the BCR4BP. The L_2 orbit possesses a saddle $\times$ saddle $\times$ center signature. To construct an initial guess using the center direction, the 6-dimensional eigenvector

Table 1. Eigenvalues associated with the dynamically equivalent orbit associated with the Earth-Moon L_1 and L_2 libration points in the BCR4BP.

λ_{L_1}	λ_{L_2}
4.275×10^{8}	7.7667×10^{5}
3.859×10^{-7}	1.2877×10^{-6}
$-0.9937 + 0.1117i$	0.6023
$-0.9937 - 0.1117i$	1.6600
$-0.9508 + 0.3098i$	$0.8657 + 0.5005i$
$-0.9508 - 0.3098i$	$0.8657 - 0.5005i$

associated with the desired center direction is computed, $\mathbf{v}_c$. Following the procedure in McCarthy and Howell,[12] the initial set of states on the invariant curve is defined,

$$\mathbf{x}_i^0 = \mathbf{x}^* + \epsilon \left(\text{Re}\left[\mathbf{v}_c\right] \cos\left(\theta_{1i}\right) - \text{Im}\left[\mathbf{v}_c\right] \sin\left(\theta_{1i}\right) \right) \tag{7}$$

where $\mathbf{x}_i^0$ is the initial guess for the i^{th} 6-dimensional state on the invariant curve, $\mathbf{x}^*$ is the 6-element state vector on the periodic orbit at the location where the monodromy matrix is computed, $\text{Re}\left[\mathbf{v}_c\right]$ and $\text{Im}\left[\mathbf{v}_c\right]$ are the real and imaginary components of the eigenvector associated with the center mode, respectively, θ_{1i} is the i^{th} latitudinal angle along the invariant curve, and ϵ is a small quantity. The last two parameters to specify a complete initial guess for a torus are the longitudinal period, T^0, and the rotation angle ρ^0. The longitudinal period is approximated as the period of the orbit. The initial approximation for the rotation angle is the angular location of the center eigenvalue on the unit circle in the complex plane,

$$\rho^0 = \tan^{-1}\left(\frac{\text{Im}\left[\lambda_c\right]}{\text{Re}\left[\lambda_c\right]}\right) \tag{8}$$

where λ_c is the center eigenvalue. Since the frequency that reflects the Sun moving along its orbit represents the longitudinal frequency for quasi-periodic orbits in the BCR4BP, each of the states on

the invariant curve possess the same Sun angle, and return to the stroboscopic map at the same Sun angle. This process yields an initial guess for the first quasi-periodic torus in the family. Using this initial guess, the GMOS algorithm is then used to compute the full torus.

Method 2: Continuation in Sun Mass from CR3BP to BCR4BP

The BCR4BP is formulated as an Earth-Moon CR3BP augmented with a periodic force from the Sun. The CR3BP has been studied by many researchers and much is known about solutions and orbits that exist in this problem. Additionally, the CR3BP is an autonomous system, thus, periodic orbits exist in families of solutions. By introducing a periodic forcing term (i.e., the Sun) to the problem, many of these CR3BP periodic orbits have a dynamically equivalent quasi-periodic orbit in the BCR4BP. To generate an initial guess, a periodic orbit in the CR3BP is transitioned to a quasi-periodic orbit by scaling up the Sun mass using the ε parameter as reflected in Equation (4). Consider an L_1 planar periodic Lyapunov orbit in the Earth-Moon CR3BP as plotted in Figure 3(a). This periodic orbit delivers a quasi-periodic equivalent in the BCR4BP. First, the states along the invariant curve are parameterized. Since the periodic orbit represents the torus when $\varepsilon = 0$, the orbit is discretized uniformly in time to represent N discretized points along the invariant curve. These points represent the invariant curve for the torus when $\varepsilon = 0$. The L_1 Lyapunov orbit in Figure 3(a) is discretized into $N = 45$ states. The states along the periodic orbit are propagated forward for one synodic period, T_{syn} which is equal to the longitudinal period. The last parameter required to fully define the torus is the rotation angle. The rotation angle is computed by determining the angle between 0 and 2π that satisfies the invariance constraint between the initial states and the states propagated to the first return on the stroboscopic map. The invariance constraint from the GMOS algorithm is formulated,

$$\mathbf{F}_{invar} = \mathbf{R}_{-\rho}\mathbf{U}^t - \mathbf{U} = \mathbf{0} \tag{9}$$

where $\mathbf{R}_{-\rho}$ is the rotation operator, $\mathbf{U}^t$ is the $N \times 6$ matrix of states at the first return to the

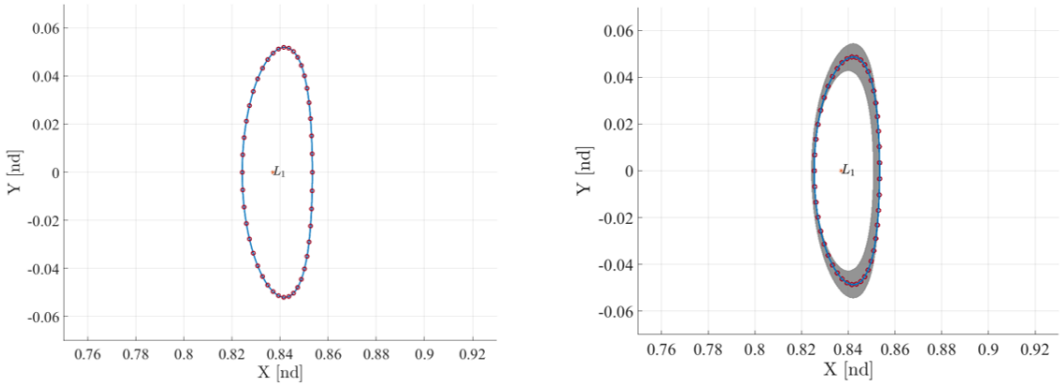

(a) (b)

Figure 3. Torus representation of a planar periodic Lyanpunov orbit when (a) $\varepsilon = 0$ and (b) $\varepsilon = 1$.

stroboscopic map, and $\mathbf{U}$ is the $N \times 6$ matrix of states on the invariant curve. The nomenclature in this definition of the invariance constraint is consistent with notation in McCarthy and Howell.[12] A root solving routine delivers a rotation angle, ρ, that resolves Equation (9) to zero. This rotation angle, satisfying the invariance constraint, defines the rotation on the torus when $\varepsilon = 0$, in the

CR3BP. The torus is now fully defined for $\varepsilon = 0$ and a pseudo-arclength continuation process transitions the solution at $\varepsilon = 0$ to $\varepsilon = 1$. The continuation algorithm is formulated using a free-variable/constraint differential corrections method for each solution. The free variable vector is defined,

$$\mathbf{X} = \begin{bmatrix} \mathbf{u}_1 & \mathbf{u}_2 & \dots & \mathbf{u}_N & \varepsilon \end{bmatrix}^T \tag{10}$$

where $\mathbf{u}_i$ is the i^{th} 6-element state vector on the invariant curve and ε is the Sun mass scaling term included in Equation (4). The free variable vector contains $6N + 1$ elements. The constraint vector is defined,

$$\mathbf{F} = \begin{bmatrix} \mathbf{F}_{\text{invar}} & F_{\theta_1} \end{bmatrix}^T \tag{11}$$

where $\mathbf{F}_{\text{invar}}$ is the invariance constraint defined in Equation (9), rearranged as a row vector, and F_{θ_1} is the scalar latitudinal phasing constraint to ensure that a new torus is computed rather than a phase shifted location around the curent invariant curve. This differential corrections strategy is extendable to a multiple shooting formulation. The details of the free variables, constraints, and gradients are summarized by McCarthy.[6] Note that the constraint vector includes $6N + 1$ elements prior to the inclusion of the pseudo-arclength constraint; however, the phase constraint is not a unique property of the torus. Consequently, including the phase constraint does not over-constrain the differential corrections problem. Also note the partial derivative of the invariance constraint with respect to ε is evaluated as,

$$\frac{\partial \mathbf{F}_{\text{invar}}}{\partial \varepsilon} = \mathbf{R}_{-\rho} \frac{\partial \mathbf{U}^t}{\partial \varepsilon} \tag{12}$$

where the $\frac{\partial \mathbf{U}^t}{\partial \varepsilon}$ is the partial derivative of the discretized states at the first return to the stroboscopic map with respect to ε. Since this partial derivative relies on the variations of the state with respect to ε, it can be approximated via finite differencing or by numerically propagating the variational equations. Numerical experiments demonstrate that finite differencing is particularly sensitive to the size of a perturbation. Consequently, the computation of the partial derivatives is not sufficiently accurately to exploit pseudo arclength continuation, as the nullspace of the Jacobian matrix is required. To avoid introducing such errors into the nullspace calculation, the variational equations of motion are propagated. The differential equations associated with the variations of the states with respect to ε are defined by augmenting the BCR4BP state variational equations,

$$\dot{\mathbf{\Phi}} = \mathbf{A}\mathbf{\Phi} = \begin{bmatrix} 0 & 0 & 0 & 1 & 0 & 0 & 0 \\ 0 & 0 & 0 & 0 & 1 & 0 & 0 \\ 0 & 0 & 0 & 0 & 0 & 1 & 0 \\ \Upsilon_{xx} & \Upsilon_{xy} & \Upsilon_{xz} & 0 & 2 & 0 & \Upsilon_{x\varepsilon} \\ \Upsilon_{yx} & \Upsilon_{yy} & \Upsilon_{yz} & -2 & 0 & 0 & \Upsilon_{y\varepsilon} \\ \Upsilon_{zx} & \Upsilon_{zy} & \Upsilon_{zz} & 0 & 0 & 0 & \Upsilon_{z\varepsilon} \\ 0 & 0 & 0 & 0 & 0 & 0 & 0 \end{bmatrix} \mathbf{\Phi} \tag{13}$$

where $\mathbf{\Phi}$ is a 7×7 matrix of the state variations, Υ_{ab} is the second partial derivative of the pseudo-potential function with respect to a and b. The pseudo-potential derivatives with respect to the state

variables and ε are defined,

$$\Upsilon_{x\varepsilon} = -m_4 \left(\frac{x - x_4}{r_{43}^3} + \frac{x_4}{a_4^3} \right) \tag{14}$$

$$\Upsilon_{y\varepsilon} = -m_4 \left(\frac{y - y_4}{r_{43}^3} + \frac{y_4}{a_4^3} \right) \tag{15}$$

$$\Upsilon_{z\varepsilon} = -m_4 \left(\frac{z - z_4}{r_{43}^3} + \frac{z_4}{a_4^3} \right) \tag{16}$$

The remaining second partial derivatives of the pseudo-potential function in the $\mathbf{A}$ matrix are derived in Boudad.[5] The continuation process proceeds until $\varepsilon = 1$. The equivalent quasi-periodic L_1 Lyapunov orbit in the BCR4BP is plotted as a grey surface and the invariant curve is plotted in blue in Figure 3(b). It is possible to compute the same orbit using Method 1; however, not all periodic orbits in the CR3BP possess an equivalent quasi-periodic analog in the BCR4BP.

$\mathbf{L_1}$ QUASI-PERIODIC ORBITS

As noted by Jorba et al., there exists an orbit in the BCR4BP that is dynamically equivalent to the L_1 libration point from the CR3BP.[9] This orbit is constructed using a continuation method to transition from an Earth-Moon CR3BP. The eigenvalues of the associated monodromy matrix are recorded in Table 1. One set of eigenvalues corresponds to planar quasi-periodic motion in the vicinity of the orbit and the second pair corresponds to out-of-plane quasi-periodic motion. The GMOS algorithm plus pseudo-arclength continuation produces the families of quasi-Lyapunov and quasi-vertical orbits. Recall that the longitudinal frequency along the torus is implicitly constrained to be the synodic frequency, so only a single phase constraint on the latitudinal frequency is required. Additionally, the free variable vector is composed of the states on the invariant curve and the rotation angle, ρ. Subsequently, the latitudinal frequency varies between each member of the family. A few members of the L_1 quasi-Lyapunov and quasi-vertical orbit families are rendered in Figure 4. Note that the quasi-vertical family retains a similar geometry to quasi-vertical orbits in the CR3BP. The stability of these orbits is computed using a stability index, ν, as defined by McCarthy and Howell, and is plotted for each family in Figure 5.[12] The members of both families are unstable since the stability index $\nu > 1$. The quasi-Lyapunov family includes a bifurcation to the L_1 quasi-halo family; the bifurcating orbit is highlighted in blue in Figure 4(a). Similar to the CR3BP, there are northern and southern quasi-halo families in the BCR4BP. Members of the northern quasi-halo family are plotted in Figure 6. These orbits offer useful information about the behavior in the vicinity of L_1.

Stepping Over Frequency Resonances

As noted by Schilder, et al., when strong resonances between the frequencies are encountered during the pseudo-arclength continuation process, a quasi-periodic orbit collapses to a periodic orbit and the continuation halts. To avoid this phenomenon, the continuation strategy switches to natural parameter continuation using the rotation angle as the stepping parameter. The frequency ratio is defined,

$$\frac{\omega_1}{\omega_2} = \frac{2\pi}{\rho} \tag{17}$$

where ρ is still the rotation angle. When a strong resonance is detected, a quasi-periodic orbit is converged before the resonance is encountered. Using the previous two members of the family, it is

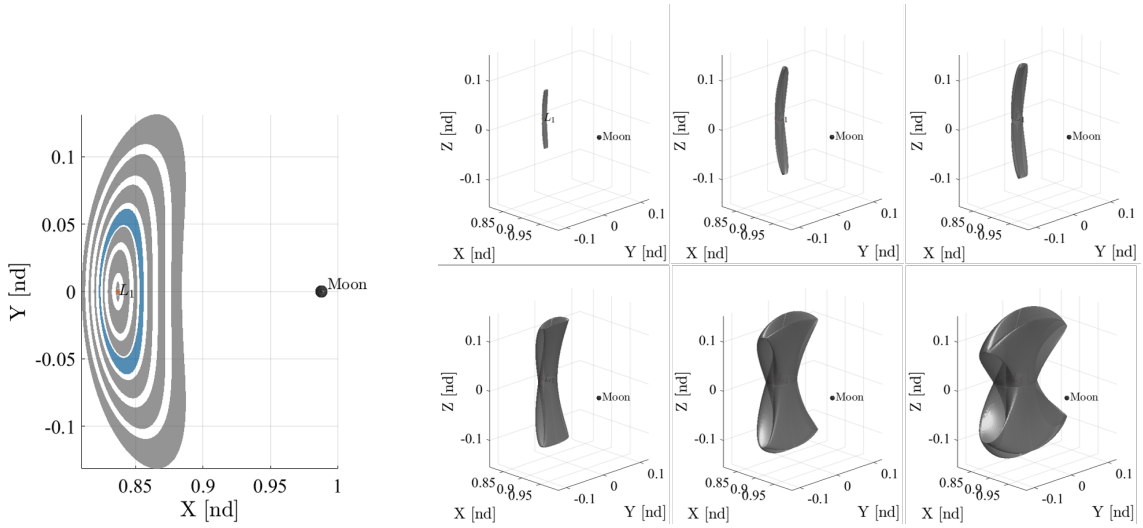

(a) (b)

Figure 4. Members of the L_1 quasi-Lyapunov family (left) and the L_1 quasi-vertical family (right). The quasi-Lyapunov orbit highlighted in blue is the bifurcating orbit to the L_1 quasi-halo family.

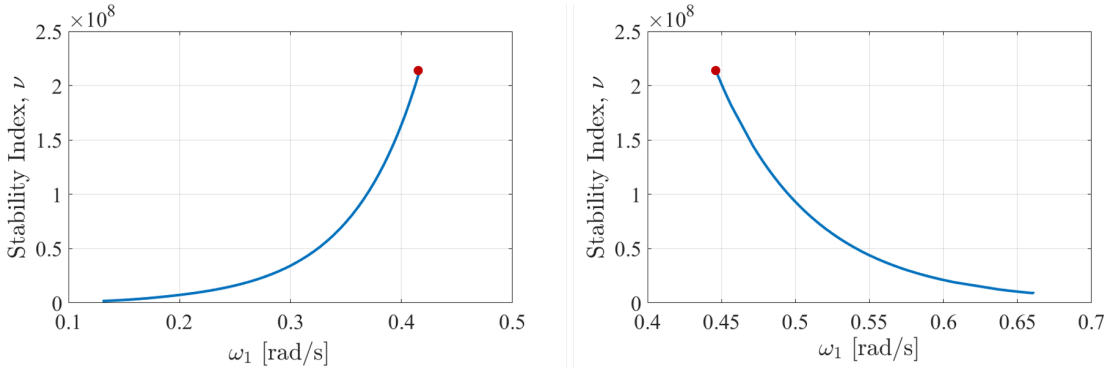

Figure 5. Stability index computed for the L_1 quasi-Lyapunov orbit family (left) and the L_1 quasi-vertical family (right). The red dot indicates the start of the family where it bifurcates from the dynamically equivalent L_1 orbit in the BCR4BP.

determined whether the rotation angle is increasing or decreasing and a rotation angle is selected for the next member in the natural parameter continuation scheme to step over the resonance. An initial guess for the quasi-periodic orbit to "step over" the resonance is formulated using this rotation angle and the states from the quasi-periodic orbit that converged prior to the resonance.

L_2 QUASI-PERIODIC ORBITS

In contrast to the libration point L_1, there is no unique dynamical equivalent for the L_2 point in the BCR4BP as the system evolves from the Earth-Moon CR3BP. As noted by Jorba-Cuscó et al. and in Figure 2(b), if the L_2 point is transitioned using homotopy from the CR3BP to the BCR4BP, it transitions to a 2:1 resonant periodic Lyapunov orbit.[15] The eigenvalues associated with this 2:1 orbit are listed in Table 1. Note that there is a single pair of complex, unit magnitude eigenvalues

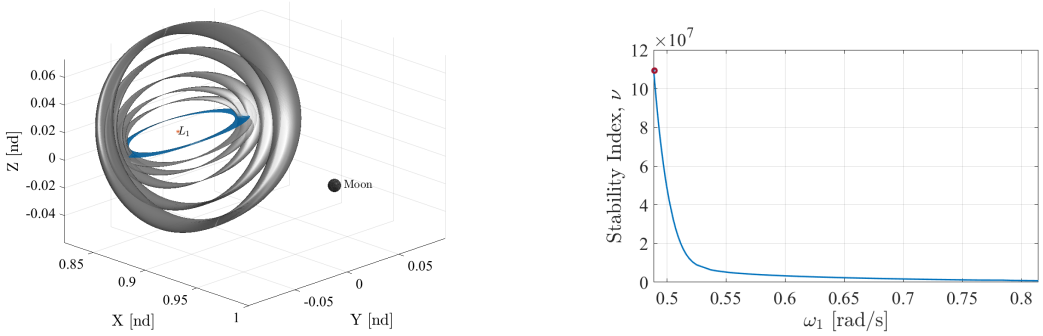

(a) (b)

Figure 6. (a) Members of the L_1 northern quasi-Lyapunov family; the bifurcating Lyapunov orbit is highlighted in blue (a). Stability index for the L_1 quasi-halo family as a function of latitudinal frequency (b). The origin of the family at the bifurcating quasi-Lyapunov orbit is indicated by the red dot.

that correspond to the planar L_2 quasi-Lyapunov family. A few members of the L_2 quasi-Lyapunov family are rendered in Figure 7. Note that members of the L_2 family, in contrast to the L_1 family, appear to all overlap with one another and the y-amplitude of the torus in configuration space increases as ρ decreases, whereas the orbits in the L_1 family emanate from the dynamically equivalent L_1 orbit. Additionally, all of the members of the L_2 quasi-Lyapunov family are unstable. Given that

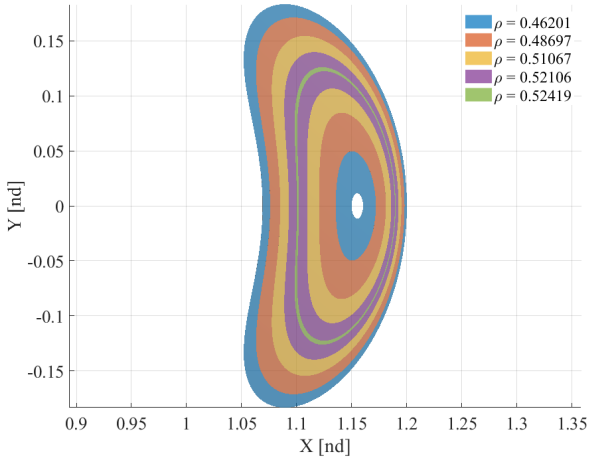

Figure 7. L_2 quasi-Lyapunov family.

the stability changes during the continuation of the CR3BP L_2 point to the BCR4BP, as noted in Figure 2(b), the precise locations of these bifurcations may be insightful. Consider the stability change where $\varepsilon = 0.287$, i.e., the stability transitions from a single saddle mode to two saddle modes. Following this bifurcation, ε returns to zero, $\varepsilon \to 0$, and the resultant dynamical structure is an L_2 halo orbit with a period equal to double the synodic period, indicating a 2:1 synodic resonance. Since the orbital period is in resonance with the synodic period, an equivalent periodic orbit in the BCR4BP ($\varepsilon = 1$) exists. After transitioning this 2:1 synodic resonant halo orbit to the BCR4BP using the

same free variable/constraint method with Equations (5) and (6), the eigenvalues associated with the monodromy matrix of the orbit are examined. The monodromy matrix possesses two complex conjugate pairs of eigenvalues, all of unit magnitude. The two families of quasi-halo orbits associated with each pair are computed and a few members of each family are plotted in Figure 8. Both quasi-halo orbit families bifurcate from the same periodic orbit, however, the characteristics of each family differ. The quasi-halo family rendered in Figure 8(a) appears similar to L_2 quasi-halo orbits in the CR3BP.[12] However, the quasi-halo family plotted in Figure 8(b) evolves to a different type of behavior than the quasi-halo motion in the Earth-Moon CR3BP. The hodograph of the rotation angle as a function of the x-component where $\theta_0 = \theta_1 = 0$ along the torus is plotted in Figure 9(b); the red dot indicates the origin of the family. An example of a trajectory arc from one of the family members is plotted in Figure 9(a); the torus associated with this trajectory is denoted by the gold dot on the plot in Figure 9(b). Note that the behavior of the quasi-periodic trajectory in Figure 9(a) appears to include Lissajous motion combined with quasi-halo arcs since solar perturbations have been introduced. This is more apparent when the $\hat{z}$-component of position is plotted as a function of time in Figure 10. The smaller oscillations in the $\hat{z}$-component indicate the Lissajous-type motion and the larger oscillations indicate the traditional quasi-halo type motion. The Subsequently, the dynamical environment near the Earth-Moon L_2 region, when perturbed by the Sun, possesses unique structured motion that can be leveraged for trajectory design.

As Rosales notes, the L_2 region is much more dynamically sensitive to solar perturbations in the BCR4BP; subsquently, solutions may be more challenging to compute by following bifurcations from the periodic 2:1 L_2 halo and Lyapunov orbits in the BCR4BP.[7] To examine other analogous structures from the CR3BP that evolve into the BCR4BP, continuation in Sun mass from the CR3BP to the BCR4BP is investigated. Consider a low amplitude L_2 periodic vertical orbit in the Earth-Moon CR3BP. Using the Sun mass continuation method, this periodic vertical orbit is transitioned from the CR3BP ($\varepsilon = 0$) to a quasi-periodic orbit in the BCR4BP ($\varepsilon = 1$). The periodic vertical orbit from the CR3BP (blue) and the corresponding quasi-vertical orbit (grey) in the BCR4BP are plotted together in the Earth-Moon rotating frame in Figure 11(a). Additionally, ε is plotted as a function of the x position coordinate when $\theta_1 = \theta_0 = 0$. The red dot indicates the low-amplitude vertical orbit in the CR3BP. Note that the curve in ε follows a similar pattern to the L_2 point continuation from Figure 2(b) where ε initially decreases to become negative, before becoming positive and transitioning to the full BCR4BP. The yellow dot highlights the continuation process as it passes through the CR3BP again ($\varepsilon = 0$). The dynamical structure in this instance is a quasi-vertical torus in the CR3BP where one of the fundamental frequencies is equal to the synodic frequency. After computing this single quasi-vertical orbit in the BCR4BP, the pseudo-arclength continuation process begins using the GMOS algorithm. A few members of the quasi-vertical family are rendered in Figure 12. Note that the flat quasi-vertical orbit (left) in Figure 12 is near the bifurcation to the quasi-Lyapunov orbit family, as noted by Rosales.[7] Using the technique for the continuation in Sun mass reveals additional properties associated with the motion in the vicinity of the Sun-perturbed L_2 region.

Transitioning solutions through continuation in Sun mass supplies useful information concerning the dynamics in the cislunar region; however, challenges arise when attempting to transition some types of solutions. The GMOS algorithm relies on a Fourier series to represent the invariant curve and an assumption associated with the Fourier series is that a reasonable number of states can represent the invariant curve via a discrete Fourier transform. When the geometry of the invariant curve becomes too complex, the number of points required to accurately represent the curve becomes in-

feasible and the continuation process cannot proceed. The limitations of formulating the invariant curve using a Fourier series are clearly highlighted.

CONCLUDING REMARKS

Since quasi-periodic orbits exist as families of solutions in the BCR4BP, examining their properties supplies insight into the Sun-perturbed environment in cislunar space. Analogous dynamical structures associated with the Earth-Moon L_1 and L_2 libration points are transitioned and examined in the BCR4BP. During the transition process of the L_2 point from the CR3BP to the BCR4BP, stability changes are encountered. One of these bifurcations leads to a 2:1 L_2 synodic resonant halo

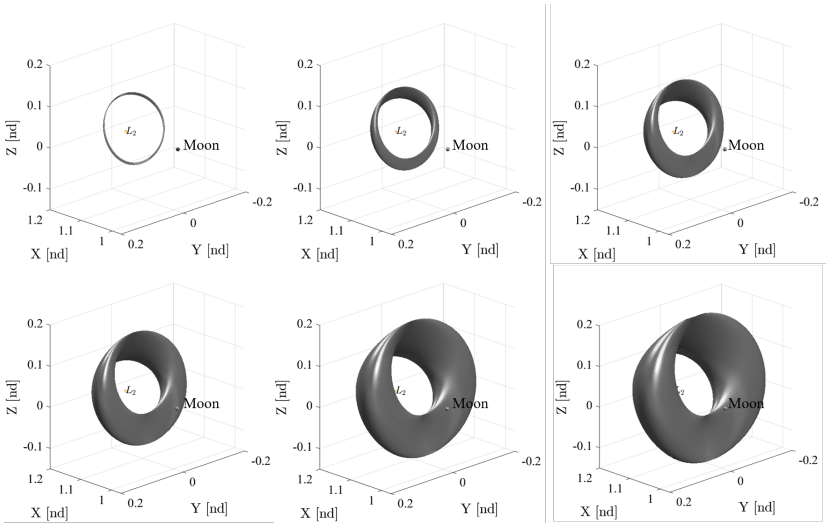

(a)

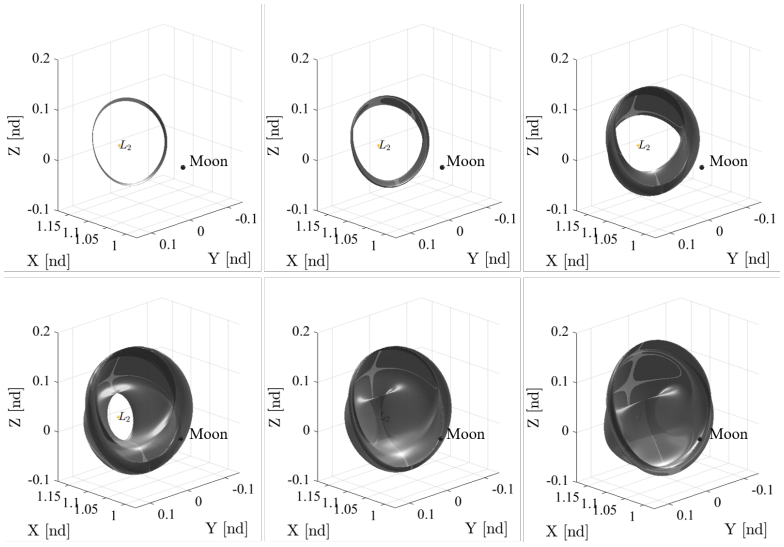

(b)

Figure 8. Members of two families of L_2 quasi-halo orbits that bifurcate from the 2:1 resonant L_2 halo orbit. The family rendered in (a) evolves toward the Moon, while the family rendered in (b) evolves away from the Moon.

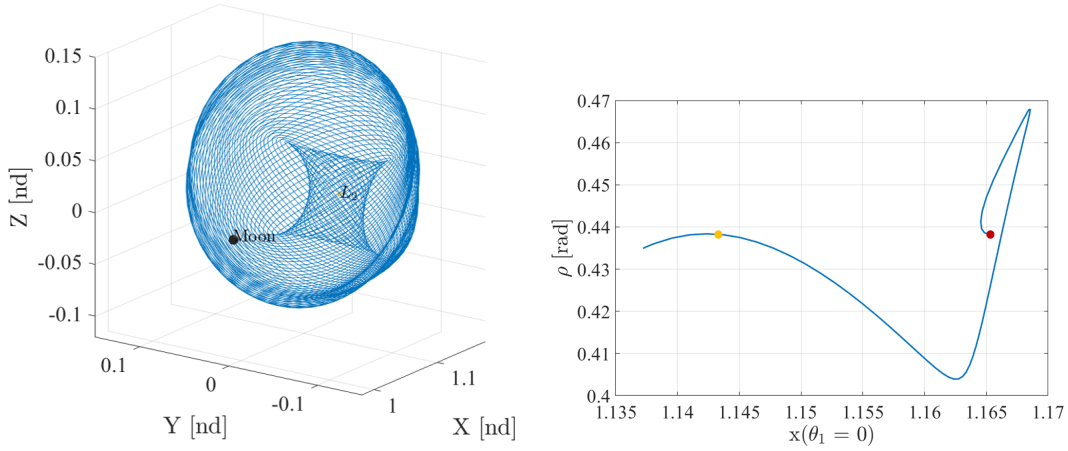

(a) (b)

Figure 9. (a) Trajectory arc propagated on an L_2 quasi-halo orbit with a rotation angle $\rho = 0.43814$. (b) Hodograph of the rotation angle vs the x-component of the torus where $\theta_0 = \theta_1 = 0$ for the quasi-halo family represented in Figure 8(b).

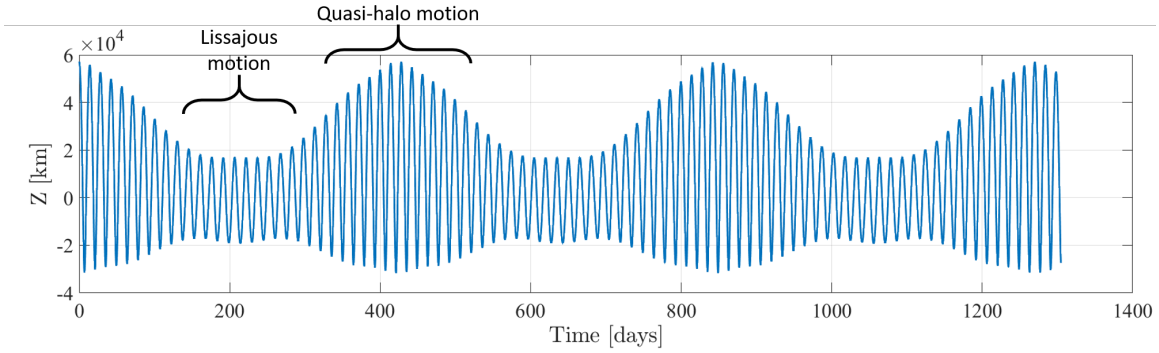

Figure 10. The $\hat{z}$-component of the trajectory from Figure 9(a) as a function of time. The trajectory is propagated for 1300 days.

orbit. Two methods are detailed to initialize a family of quasi-periodic tori in the BCR4BP. The first approach exploits the center subspace of a periodic orbit to initialize a torus. The second method attempts to exploit the pseudo-arclength continuation process that transitions a periodic orbit in the CR3BP to the BCR4BP. Not all periodic orbits in the CR3BP transition directly into the BCR4BP and, particularly when the invariant curve possesses a complex geometry, the GMOS algorithm and continuation process encounter challenges. Families of solutions for quasi-Lyapunov, quasi-halo, and quasi-vertical orbits are investigated in the vicinity of L_1 and L_2, however, more solutions exist in the cislunar region. Understanding this fundamental motion provides trajectory designers with a wider array of options for preliminary path planning. Including the Sun in the preliminary model introduces unique quasi-periodic structures that expand available options for path planning as well as a broader array of potential destinations in cislunar space.

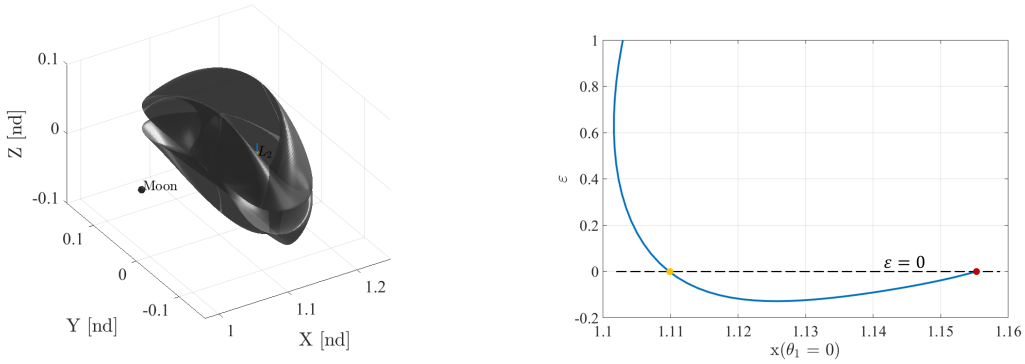

(a) (b)

Figure 11. A low amplitude periodic vertical orbit from the CR3BP (blue) that is transitioned to a quasi-vertical orbit in the BCR4BP (grey) (a). The Sun mass scaling parameter, ε, plotted as a function of the x-component of each torus where $\theta_0 = \theta_1 = 0$ through the continuation process.

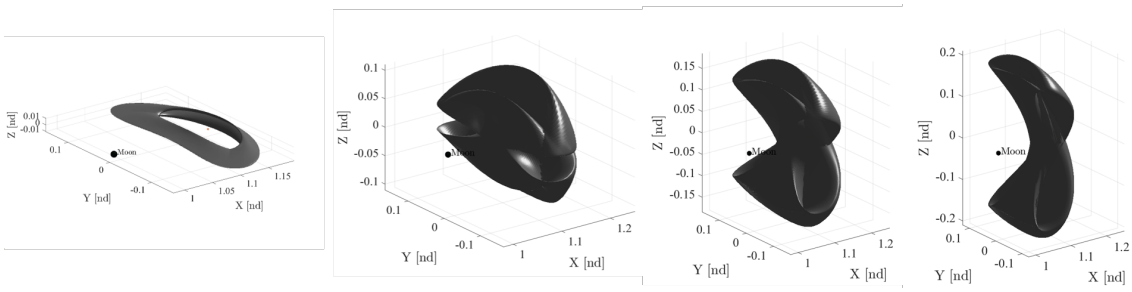

Figure 12. Members of the L_2 quasi-vertical family.

ACKNOWLEDGEMENTS

The authors would like to thank the Purdue University College of Engineering as well as the School of Aeronautics and Astronautics, as well as the Rune and Barbara Eliasen Visualization Laboratory for facilities and financial support. The authors would also like to thank the Purdue Multi-Body Dynamics Research Group, specifically Kenza Boudad and Stephen Scheuerle, for insightful discussions about the BCR4BP and formulating pseudo-arclength continuation in the BCR4BP.

REFERENCES

[1] National Aeronautics and Space Administration, "NASA's Lunar Exploration Program Overview," Sept. 2020.

[2] D. C. Davis, K. K. Boudad, S. M. Phillips, and K. C. Howell, "Disposal, Deployment, and Debris in Near Rectilinear Halo Orbits," *29th AAS/AIAA Space Flight Mechanics Meeting*, Ka'anapali, Maui, Hawaii, Jan. 2019.

[3] S. T. Scheuerle, B. P. McCarthy, and K. C. Howell, "Construction of Ballistic Lunar Transfers Leveraging Dynamical Systems Techniques," *AAS/AIAA Astrodynamics Specialist Virtual Conference*, Lake Tahoe, California, Aug. 2020.

[4] B. P. McCarthy and K. C. Howell, "Cislunar Transfer Design Exploiting Periodic and Quasi-Periodic Orbital Structures in the Four-Body Problem," *71st International Astronautical Congress*, Virtual, Oct. 2020.

[5] K. K. Boudad, "Disposal Dynamics From the Vicinity of Near Rectilinear Halo Orbits in the Earth-Moon-Sun System," MS Thesis, Purdue University, West Lafayette, Indiana, Dec. 2018.

[6] B. P. McCarthy, "Characterization of Quasi-Periodic Orbits for Applications in the Sun-Earth and Earth-Moon Systems," MS Thesis, Purdue University, West Lafayette, Indiana, Dec. 2018.

[7] J. J. Rosales, *On the Effect of the Sun's Gravity Around the Earth-Moon L_1 and L_2 Libration Points*. Ph.D. Dissertation, Universitat de Barcelona, Barcelona, Spain, June 2020.

[8] A. Jorba and J. Villanueva, "On the Persistence of Lower Dimensional Invariant Tori Under Quasi-Periodic Perturbations," *Journal of Nonlinear Science*, Vol. 7, No. 5, 1997, pp. 427–473.

[9] A. Jorba, M. Jorba-Cuscó, and J. Rosales, "The vicinity of the Earth-Moon L1 point in the Bicircular Problem," *Celestial Mechanics and Dynamical Astronomy*, Vol. 132, Feb. 2020.

[10] A. Jorba and B. Nicolás, "Transport and invariant manifolds near L3 in the Earth-Moon Bicircular model," *Communications in Nonlinear Science and Numerical Simulation*, Vol. 89, Sept. 2020.

[11] E. Castella and A. Jorba, "On the Vertical Families of Two-Dimensional Tori Near the Triangular Points of the Bicircular Problem," *Celestial Mechanics and Dynamical Astronomy*, Jan. 2000, pp. 35–54.

[12] B. P. McCarthy and K. C. Howell, "Leveraging Quasi-Periodic Orbits for Trajectory Design in Cislunar Space," *Astrodynamics*, Vol. (Available Online), Jan. 2021.

[13] G. Gomez and J. M. Mondelo, "The Dynamics Around the Collinear Equilibrium Points of the RTBP," *Physica D: Nonlinear Phenomena*, Vol. 157, Oct. 2001, pp. 283–321.

[14] Z. P. Olikara and D. J. Scheeres, "Numerical Methods for Computing Quasi-Periodic Orbits and Their Stability in the Circular Restricted Three-Body Problem," *IAA Conference on Dynamics and Control of Space Systems*, Porto, Portugal, Mar. 2012.

[15] M. Jorba-Cuscó, A. Farrés, and A. Jorba, "Two Periodic Models for the Earth-Moon System," *Frontiers in Applied Mathematics and Statistics*, Vol. 4, July 2018.